**Channel response to sediment release: insights from a paired analysis of dam removal**

Mathias J. Collins[1*], Noah P. Snyder[2], Graham Boardman[3], William S.L. Banks[4], Mary Andrews[5], Matthew E. Baker[6], Maricate Conlon[7], Allen Gellis[8], Serena McClain[9], Andrew Miller[6], Peter Wilcock[10]

[1] Restoration Center, National Marine Fisheries Service, National Oceanic and Atmospheric Administration, Gloucester, MA

[2] Department of Earth and Environmental Sciences, Boston College, Chestnut Hill, MA

[3] Stantec, Baltimore, MD

[4] Colorado Water Science Center, US Geological Survey, Pueblo, CO

[5] Restoration Center, National Marine Fisheries Service, National Oceanic and Atmospheric Administration, Annapolis, MD

[6] Department of Geography and Environmental Systems, University of Maryland—Baltimore County, Baltimore, MD

[7] Fleming-Lee Shue, Inc., New York, NY

[8] Maryland, Delaware, D.C. Water Science Center, US Geological Survey, Baltimore, MD

[9] American Rivers, Washington, DC

[10] Department of Watershed Sciences, Utah State University, Logan, UT

* Corresponding author: National Marine Fisheries Service, National Oceanic and Atmospheric Administration, 55 Great Republic Drive, Gloucester, MA, 01930, USA; mathias.collins@noaa.gov

**KEY POINTS**

- Erosion response to dam removal sediment release is two-phased with exponentially decreasing rates characterizing both phases
- Changing decay constants are associated with a process shift from rapid erosion driven by base level change to episodic erosion requiring floods
- Valley width influences the rate and completeness of impoundment sediment evacuation

**ABSTRACT**

Dam removals with unmanaged sediment releases are good opportunities to learn about channel response to abruptly increased bed material supply. Understanding these events is important because they affect aquatic habitats and human uses of floodplains. A longstanding paradigm in geomorphology holds that response rates to landscape disturbance exponentially decay through time. However, a previous study of the Merrimack Village Dam (MVD) removal on the Souhegan River in New Hampshire, USA, showed that an exponential function poorly described the early geomorphic response. Erosion of impounded sediments there was two-phased. We had an opportunity to quantitatively test the two-phase response model proposed for MVD by extending the record there and comparing it with data from the Simkins Dam removal on the Patapsco River in Maryland, USA. The watershed sizes are the same order of magnitude ($10^2$ km$^2$), and at both sites low-head dams were removed (~ 3-4 m) and ~65,000 m$^3$ of sand-sized sediments were discharged to low-gradient reaches. Analyzing four years of repeat morphometry and sediment surveys at the Simkins site, as well as continuous

discharge and turbidity data, we observed the two-phase erosion response described for MVD. In the early phase, approximately 50% of the impounded sediment at Simkins was eroded rapidly during modest flows. After incision to base level and widening, a second phase began when further erosion depended on floods large enough to go over bank and access impounded sediments more distant from the newly-formed channel. Fitting functional forms to the data for both sites, we found that two-phase exponential models with changing decay constants fit the erosion data better than single-phase models. Valley width influences the two-phase erosion responses upstream, but downstream responses appear more closely related to local gradient, sediment re-supply from the upstream impoundments, and base flows.

Keywords: dam removal, erosion, channel evolution, fluvial geomorphology, deposition

## Introduction

Understanding how rivers respond to natural and anthropogenic increases in sediment supply is important because these disturbances impact the biota and human uses of channel and floodplain environments. A long-standing hypothesis in geomorphology is that fluvial response rates to disturbance generally exhibit continuous exponential decay (*Graf*, 1977). In the context of a sudden increase in sediment supply (e.g., a landslide), erosion rates would be expected to decline over time as a function of the quantity of sediment remaining. A continuous exponential decay of the response rate implies that the processes controlling erosion remain largely the same throughout the response period.

In contrast, a recent dam removal study in the Northeast United States found that erosion of noncohesive sediment from the de-watered reservoir exhibited a two-phase response (*Pearson et al.*, 2011). *Pearson et al.* (2011) proposed that erosion of impounded sediment is first driven by the local increase in energy gradient caused by the base level lowering with dam removal. Later, after incision to the new base level and some widening to accommodate relatively small, frequent flows, larger flood events are necessary to erode impounded sediments more distant from the new channel. Adapting terms introduced by *Pizzuto* (2002) in the context of dam removal, *Pearson et al.* (2011) described the early phase driven by base level change as "process-driven" and the later phase requiring floods as "event-driven". They suggested that the change in controlling processes was indicated by the failure of a single-phase exponential decay model to describe the observed erosion rates. *Major et al.* (2000) and *Gran et al.* (2011), studying sediment yield response to disturbance from volcanic eruptions, also found single-phase exponential decay models insufficient to describe rates because of changing processes during the response. Dynamic controls on erosion and sedimentation have been observed in other circumstances that produce abrupt increases in sediment supply to rivers such as mass wasting (e.g., *Kieffer*, 1985; *Webb et al.*, 1999; *Larsen et al.*, 2004).

We had an opportunity to test the two-phase erosion-response model proposed by *Pearson et al.* (2011) by investigating a dam removal that shares many important characteristics with their Merrimack Village Dam (MVD) removal site on the Souhegan River, New Hampshire: the 2010 removal of Simkins Dam on the Patapsco River in Maryland. The watershed sizes are the same order of magnitude ($10^2$ km$^2$), and both dams were relatively low head (~ 3-4 m) and impounded ~65,000 m$^3$ of predominantly sand-sized sediment that was discharged to low-

gradient reaches immediately downstream. If the proposed two-phase model is true, we should see the same governing processes and style of response at the Patapsco site—potentially modulated by differences we document in valley morphology and hydrologic response. We quantitatively evaluated this by fitting functional forms to the data for each site and comparing them between sites. These analyses were compelling because data from dam-removal studies published subsequent to the Pearson et al. (2011) proposal, although not formally investigating it, conceptually support the two-phase erosion-response model and suggest it may be a general phenomenon (*Major et al.*, 2012; *Bountry et al.*, 2013; *East et al.*, 2015, *Magilligan et al.*, 2015).

**Study Areas**

The Patapsco River drains a 950 km$^2$ watershed west of Baltimore, MD (Figure 1). Much of the basin is characterized by the rolling, dissected terrain of the Maryland Piedmont with maximum watershed elevations of about 300 m (*Hack*, 1960; *Smith and Wilcock*, 2015). Within our study area the Piedmont meets the Atlantic Coastal Plain at the Fall Line, an important regional physiographic contact where hydrogeomorphic characteristics change relatively abruptly. Above the Fall Line, the Patapsco River is gravel-bedded and flowing close to bedrock in a relatively steep, incised, and confined valley (*Costa*, 1975; *MDNRWS*, 2005). The channel bed gradients in free-flowing Piedmont reaches of our study area are about 0.002. Downstream in the Coastal Plain, the channel bed is lower gradient (0.0004), unconfined, and the sand-bedded Patapsco River channel is formed in unconsolidated Quaternary sediments that thicken away from the Fall Line to about 100 m thick where the river discharges to Chesapeake Bay (*Cleaves et al.*, 1968;

*McGreevy and Wheeler*, 1985). The Fall Line also marks a bordering land use contrast: the Piedmont section flows through the lightly developed Patapsco Valley State Park whereas the tidally influenced, alluvial bottoms of the Coastal Plain section are more closely bound by urban development.

The Baltimore region climate is humid subtropical (Cfa in the Köppen classification system; (*Peel et al.,* 2007)). Annual precipitation at Baltimore Washington International Airport, less than 15 km from the study area, is about 1065 mm and relatively evenly distributed throughout the year (1981-2010 climate normal; http://www.ncdc.noaa.gov/cdo-web/datatools/normals). The Patapsco River annual hydrograph is characteristic of northeastern U.S. rivers: the highest daily median streamflows are associated with the late-winter/spring runoff period and the lowest flows occur in August through early October. Floods are generated by variety of mechanisms throughout the year including winter-spring mid-latitude cyclones, convective rainfall, and tropical cyclones (*Miller,* 1990; *Smith et al.*, 2010, 2011). Although not operated for flood control or hydropower, study site discharges are affected by storage and diversion at Liberty Reservoir (Figure 1), a municipal water supply for the city of Baltimore completed in 1956, and two additional water supply diversions. Average annual discharge for the post-1956 period at USGS gage 01589000 (Patapsco River at Hollofield, MD, hereafter "Hollofield"; Figure 1), a station about 6 km upstream of the monitoring reach with a record beginning in 1944 and some missing years between 1992 and 2010, is approximately 4.7 $m^3$/s and the mean annual flood is about 240 $m^3$/s. The years since our study began in late 2010 have been wetter: average annual discharge was about 6.5 $m^3$/s and the mean annual flood was 375 $m^3$/s. Further downstream near Simkins Dam where the watershed area increases by about 6%, continuous discharge data at USGS gage

01589025 (Patapsco River near Catonsville, MD, hereafter "Catonsville"; Figures 1 and 3b) from late 2010 to present indicate an average annual discharge of about 7.5 $m^3$/s and a mean annual flood of approximately 400 $m^3$/s (Table 1).

The ~3 m high Simkins Dam was removed from the lower Patapsco River in late fall 2010 to improve public safety, aquatic habitat, and migratory fish passage (Figures 1 and 2, Table 1). An estimated 67,000 $m^3$ of predominantly sand and some gravel in the former reservoir were released to the downstream reach that extends about 20 river km to Chesapeake Bay. The stored sediment quantity is based on estimates made by Interfluve, Inc. (unpublished data, 2009) and *Stillwater Sciences* (2010) from the geometry of the impoundment and assumptions about the pre-dam channel bed slope. Less than a kilometer downstream of Simkins Dam is the ~10 m high Bloede Dam with an impoundment that is filled with an estimated 240,000 $m^3$ of predominantly sand and mud-sized sediments with some gravel (Figure 3a and b). The Bloede impoundment creates a low-gradient, depositional reach that is uncharacteristic of the Piedmont section below Simkins Dam. Planning for the removal of Bloede Dam and release of impounded sediments is ongoing.

The Patapsco River channel in the study area is wadable at average flows. Active channel widths in free-flowing reaches range from about 25 to 50 m in both the Piedmont and Coastal Plain. Piedmont reaches are confined: the narrowest areas like the Simkins impoundment have valley widths of about 100 m while some areas near the Fall Line are closer to 300 m wide (Figure 3). Some unimpounded sections have bedrock control in places and may be non-alluvial, especially downstream of dams. Pre-removal surveys of free-flowing reaches show median grain sizes ($D_{50}$) are typically in the pebble range (4-64 mm) and occasionally in the cobble range (64-256 mm) below dams (Udden-Wentworth classification

(*Wentworth*, 1922)). The 84$^{th}$ percentile grain size (D$_{84}$) does not exceed cobble size, although boulders (> 256 mm) may be present. In the unconfined Coastal plain, the channel bed D$_{50}$ is typically in the coarse to very coarse sand range (0.5-2 mm) with D$_{84}$ not exceeding pebble size.

The MVD site, described in greater detail by *Pearson et al.* (2011), shares a number of important characteristics with the Simkins Dam removal (Table 1): drainage area order of magnitude; dam height and type; quantity and caliber of released sediments; and a low-gradient reach immediately downstream. Though New Hampshire has a humid continental climate (Köppen Dfb) characterized by large seasonal temperature differences, the annual precipitation regime and annual hydrograph seasonality are similar. Like the Mid-Atlantic, New England has multiple flood-generating mechanisms and events can occur any time of year (*Collins et al.*, 2014).

Differences between the sites relevant to this study are valley morphology and hydrologic response (Table 1). In contrast to the Simkins site, the glaciated Souhegan valley is unconfined at the project site because it is within a much larger mainstem valley just before it discharges to the Merrimack River. The differences in valley confinement are evident in the respective impoundment widths. The Simkins impoundment has a maximum wetted width only slightly wider than maximum channel widths in free-flowing reaches of the Patapsco study area. The maximum wetted width of the MVD impoundment is nearly 65% greater than Simkins. Pre-impoundment channel bed gradients local to the dams upstream also differ with Simkins being steeper (Table 1).

The Patapsco River is flashier than the Souhegan River and has a larger mean annual flood (Table 1). Using daily mean discharge data from the gages

nearest each dam (Patapsco River near Catonsville and Souhegan River at Merrimack; see Methods), we computed a Richards-Baker flashiness index for the Patapsco that is 70% greater than the Souhegan for the 1,221 days each site was monitored post-removal (*Baker et al.*, 2004). The greater flashiness at the Patapsco River likely reflects the more dense drainage network developed in the unglaciated Piedmont (Table 1) as well as other surface geology and land-use factors. The Patapsco River is also subject to modestly more intense, and higher magnitude, rainfall events (*Hershfield*, 1961; *Bonnin et al.*, 2006; *DeGaetano et al.*, 2011).

The Souhegan River, on the other hand, has a greater average annual discharge and larger base flows (Table 1). We estimated base flow magnitudes as August median flows within the 1,221-day post-removal periods (*Reis*, 1997).

**Methods**

To quantify the rates and styles of channel response to the Simkins Dam removal, we conducted pre- and post-removal channel morphometry surveys, bed sediment sampling, and continuous gaging of discharge and turbidity (Figure 4). To enable site comparisons, data collection and analytical methods, described below, were similar to those employed by *Pearson et al.* (2011). *Pearson et al.* (2011) presented two years of post-removal data collected at MVD (2008-2010). Here we extend the MVD post-removal data series by an additional four years.

*Simkins site: channel morphometry*

We conducted repeat topographic and bathymetric surveys pre- and post-removal at 28 monumented cross-sections (Figure 3b and c and Figure 4). Two control sections, XS-RA and XS-RB, are above the Simkins impoundment (Figure

3a). Surveys were completed with Topcon GPT-3000, Trimble S3, or Trimble S6 total stations with approximately 2 mm relative vertical accuracies. Horizontal control in Maryland State Plane, NAD83, was established with a Trimble R8 GPS unit with RTK/VRS correction. Estimated horizontal accuracy is about 10 mm.

Cross-sections were surveyed once before and six times after removal (Figure 4). Post-removal survey frequency was greatest in the first year after removal (three surveys in 2011) to document rapidly changing conditions in the winter and spring and the response to a large flood event on September 7 associated with Tropical Storm Lee. We estimate that event had a recurrence interval of approximately 10-years based on the Hollofield annual flood series. Survey frequency progressively decreased in successive years. Survey points were taken at significant slope breaks, edge of water, and at locations delimiting significant geomorphic features such as bars, bank toes, bank tops, etc. To supplement the quantitative data, we took repeat photographs at fixed azimuths up-, down-, and cross-stream from each cross-section monument and at over 60 additional fixed stations in the monitoring reach (not shown). Repeat photos were taken contemporaneously with cross-section survey campaigns.

Five sub-reaches where we expected the greatest geomorphic change were surveyed at a higher spatial resolution once pre- and five times post-removal to develop digital elevation models (DEMs). DEM areas included the Simkins and Bloede impoundments and three sub-reaches near the Fall Line (upstream of XS-13; above XS-14 to below XS-16; and from XS-19 to XS-21; Figure 3b and c). DEM surveys were temporally associated with, but lagging, cross-section and sediment survey campaigns (Figure 4). Surveys in the DEM areas were accomplished by establishing a series of cross-sections every 15 m and taking survey points along

these using the same instrumentation employed for the 28 monumented cross-sections. Where appropriate, locations between, and surrounding, these cross-sections were also surveyed. Cross-sections in DEM areas were staked and georeferenced for re-occupation in subsequent surveys. One exception to our DEM survey method was the 2010 pre-removal survey of the Simkins and Bloede impoundments: at that time, deeper areas of the impoundments were surveyed using a boat-mounted Sontek RiverSurveyor M9. Accuracy of the M9 is within 1% of measured depth with horizontal positioning through communication with the Trimble R8 RTK GPS. These data were merged with total-station surveys of shallow areas and banks during post-processing.

*Simkins site: streambed sediment sampling*

We evaluated bed-sediment grain-size distribution over areas extending about 7.5 m upstream and downstream of each monumented cross-section. Within these areas, we visually identified and field mapped discrete regions of relatively homogeneous sediment textures (i.e., facies) and subsequently sampled each facies for quantitative analyses. Mapping and sampling was done in relatively shallow, clear water when the bed material was visible. We employed facies mapping to evaluate bed-sediment grain-size distribution because the texture disparities between impounded sediments (predominantly sand-sized) and channel beds of Piedmont receiving reaches suggested there could be considerable substrate patchiness at downstream cross-sections after dam removal that would not be well described by a single grain-size distribution. Post-removal sampling justified this assumption.

For coarse-grained facies dominated by materials larger than granules ($D_{50}$ = 4 mm), determined visually, we used Wolman pebble counts (minimum 150) to

quantify the grain size distribution. Pebble counts were conducted in water depths generally less than 0.3 m. Finer facies (i.e., sand dominated) were bulk sampled to a depth of about 0.3 m below the bed and subsequently dry sieved in the lab. There was one pre- and five post-removal field campaigns when facies maps and grain size sampling were completed in association with cross-section surveys (Figure 4).

Nearly all facies were quantitatively sampled at one or more locations where they occurred during each field campaign. Grain size distributions for facies with multiple samples were averaged and used to represent the composition of the same facies at other locations where they occurred, but were not sampled, during the same campaign. The facies maps for each campaign were digitally rendered in a geographic information system (GIS), the percent of the cross-section occupied by each facies was computed, and the $D_{50}$ for the spatially dominant facies at a cross-section was used to represent the cross-section texture for that period. A spatially weighted average of the $D_{50}$ for all facies at a cross-section was considered as an alternate means to represent cross-section texture, but we ultimately rejected this approach (with one exception noted below) because the range of textures between facies was frequently large and resulted in unrepresentative composite distributions. Spatially dominant facies were more representative. There were four instances when no quantitative samples were available for a dominant facies. We used the $D_{50}$ of the next dominant facies for three of these occurrences because they had areal coverages within 5% of the dominant facies. For the remaining instance, we simply averaged the median grain sizes of the two other mapped facies at the section.

We also sampled the sediments impounded by Simkins Dam to estimate dry bulk density for sediment budget calculations. Surficial sediment plugs were taken from the impoundment on November 29, 2010, just days after the dam breach and

impoundment dewatering. Four samples were taken from an exposure on river left

just upstream of the dam, both upstream and downstream of the Thistle Creek

confluence (Figure 3b). The samples were obtained by driving a three-inch (~8 cm)

diameter PVC ring flush with the surface. The ring was then carefully removed to

prevent sediment loss and samples were placed in airtight bags to be transported to

the laboratory where they were desiccated and weighed using a scale with 0.01-g

precision. The dry mass of sample was then divided by its volume to determine the

dry bulk density ($\rho_{dry}$). Average bulk density for the four samples was 1.43 g/cm$^3$

(range: 1.29 to 1.53 g/cm$^3$). The impounded sediment was relatively homogeneous

in both the horizontal and vertical directions (Richard Ortt, personal communication;

Interfluve, Inc., unpublished data, 2009), similar to that observed using a more

detailed bulk density sampling strategy at MVD (*Pearson et al.*, 2011).

*Simkins site: discharge and turbidity gaging*

Discharge and turbidity data were collected at three gage sites beginning in

October 2010 (Figure 4): above the project reach (Figure 1), below the Simkins site,

and approximately 5 river kilometers below Bloede Dam near XS-16 (Figure 3b and

c). The Hollofield gage upstream of the study area was restarted on October 1, 2010,

in association with this study. On the same date the Catonsville gage and USGS

gage 01589035 (Patapsco River near Elkridge, MD, hereafter "Elkridge") were

established in the reach below Simkins Dam. At these stations discharge is

estimated by standard USGS methods from stage measurements every 15 minutes

(*Rantz*, 1982). Turbidity is also measured every 15-minutes using a Forest

Technology Systems DTS-12 turbidity sensor. The sensor reports nephelometric

turbidity units (NTU) with a dynamic range between 0 and 1,600 NTU. Discharge and

turbidity data are publicly available for each site
(http://dx.doi.org/10.5066/F7P55KJN).

*Simkins site: estimating a bed material budget*

We estimated a bed material budget to document the fate of the impounded
sediment mass in the project area and estimate rates of upstream and downstream
channel response and recovery. The budget tracks only the size fractions
represented in the bed of the impoundment and downstream that were mobile during
the project period (predominantly sand and gravel traveling as bed load with some
sand intermittently in suspended load). Mud-sized sediments were not well
represented in the bed or banks of our study and thus are not included, although we
separately quantified turbidity, as described above, and analyzed this separately. We
limited the bed material budget to the Simkins impoundment and the area
downstream to Bloede Dam because this geographic area, with its relatively short,
low gradient downstream reach, provides the best analog to the MVD case study
(Figure 3b).

The bed material budget includes watershed inputs to the Simkins
impoundment, changes in storage in the Simkins impoundment ($\Delta S_{us}$), changes in
storage from the former Simkins Dam to the Bloede Dam ($\Delta S_{ds}$), and output over the
Bloede Dam spillway as:

$$\text{Input} = \Delta S_{us} + \Delta S_{ds} + \text{Output} \tag{1}$$

This equation was applied to the intervals between each survey campaign,
defined by their respective end dates. Changes in storage between successive

surveys were estimated via repeat morphometry surveys using a combination of the monumented cross-sections and DEMs (Section 3.1). For example, the Simkins impoundment extends upstream of XS-1 for a distance of about 230 m while its extent downstream is covered by a DEM (Figure 3b). Thus, to estimate $\Delta S_{us}$ we had to: (1) difference successive XS-1 surveys and extrapolate the change in cross-sectional area at that location by multiplying it over the upstream channel centerline distance to estimate volumetric change; (2) difference successive DEMs; and (3) add the two volumetric change estimates to obtain a total volume, which was converted to mass via our bulk density estimate. $\Delta S_{ds}$ for each time interval was computed similarly by combining DEM differencing with cross-section extrapolations for the free-flowing channel not covered by the Bloede impoundment DEM (Figure 3b). DEM surveys cover approximately 80% and 40% of the $\Delta S_{us}$ and $\Delta S_{ds}$ storage areas, respectively. An exception to this general procedure was necessary for the February 2011 campaign when there were no DEM area surveys (Figure 4). The $\Delta S_{us}$ and $\Delta S_{ds}$ estimates for that time period were computed from cross-section extrapolations only. This also affected the computation of $\Delta S_{us}$ and $\Delta S_{ds}$ for the succeeding April 2011 survey because DEMs from that campaign had to be differenced from the September 2010 DEM. Thus, to determine the incremental storage changes from February 2011 to April 2011, it was necessary to subtract the storage change computed from the February 2011 campaign (this also affected our estimated uncertainties; see below and Table 2, note b).

No quantitative estimates are available for sediment quantity entering the study reach, so we used an estimate by *Stillwater Sciences* (2010) for a modeling study of the dam-removal sediment release. They used a "zeroing" run, where sediment supply is adjusted until the model produces a longitudinal profile similar to

that observed, to estimate an input of approximately 4,000 m$^3$/yr, or about 5,700 t/yr at a bulk density of 1.43 g/cm$^3$. Outputs over Bloede Dam were not measured directly but were residual calculations via Equation 1. We also estimated changes in storage in the Piedmont reach immediately below Bloede Dam from measurements of cross-sectional area changes at XS-9 through XS-16 that were extrapolated as described above (Table 2, last column). Although not a perfect analog for material passing over the dam at a given time considering simultaneous erosion and downstream transport in this comparatively long reach, these estimates provide a check on the residual calculations that accumulate, and hide, all errors associated with each component of the sediment budget (*Kondolf and Matthews*, 1991). The calculated outputs over Bloede Dam compare reasonably well with the estimated downstream storage changes based on measurements, considering the estimated uncertainty (described below), affording us a degree of confidence in our budget estimates.

We estimated measurement errors for our storage terms by computing root mean square error (RMSE) for cross-section surveys and DEMs and propagating errors using standard methods (*Taylor*, 1997). Because our measurement errors include both independent, random errors that we could explicitly estimate and systematic errors we could not, we accounted for both sources by propagating errors more conservatively as ordinary sums rather than in quadrature (*Taylor*, 1997; *Grams et al.*, 2013). Systematic measurement errors include different survey instrument types used for the first DEM surveys, estimated locations for upstream impoundment limits, and channel centerline representations of true centerlines for a given survey campaign. Random measurement errors estimated below are 95% confidence estimates (i.e., 2 * RMSE). These do not include uncertainties associated

with estimating volume changes over unsurveyed channel reaches from cross-section extrapolations because measuring this kind of model uncertainty is difficult to do precisely and requires field calibration (*Grams et al.*, 2013).

Because final morphometry data for each technique include errors from field data collection and post-processing, we estimated RMSEs as follows. For the cross-section surveys, we computed the area difference between successive, processed surveys at the control sections for the September 2010 to February 2011 survey interval when elevation changes should have been zero. For the DEM surveys, we computed the volume difference between successive, processed surveys at DEM 1 for the September 2010 to April 2011 survey interval when elevation changes should have been zero. Absent a means to estimate the measurement error for the one instance of hydroacoustic surveys (September 2010 impoundment DEMs), we assumed the same measurement error as the total station DEM surveys. When extrapolating cross-section area changes over channel distances upstream and/or downstream to estimate volume changes, we estimated a 2% random error in channel distance measurements made using a channel centerline GIS shapefile and supplemental on-screen digitizing. This estimate was computed from the standard deviation of repeat on-screen digitizing measurements of typical distances. On-screen digitizing was only necessary over short distances from centerline nodes, between which the GIS computed exact distances (with unknown bias). We estimated the error in our bulk density estimate (3.5%) as the standard error of the four measurements used to compute the mean bulk density. Random error for cross-section surveys is estimated as 3.1 $m^2$ (~ 0.1 m elevation) and for DEMs as 1090 $m^3$.

*MVD site*

As noted, the methods employed at MVD to document channel response to dam removal were the model for the Simkins study. Channel morphometry changes over the smaller study area at MVD (~1 km) were documented by detailed total-station surveys of 12 monumented cross-sections and associated repeat photos. Bed sediment grain-size distribution changes over time were assessed by bulk sampling sand-sized and finer sediments and subsequent analyses in the lab. Cross-sections dominated by coarser sediments were characterized by Wolman pebble counts. Continuous discharge for the Souhegan River was measured ~ 1 km upstream of the MVD study area at USGS gage 01094000 (Souhegan River at Merrimack, NH), a station with over 100 years of record (1909 to present).

We did not collect continuous turbidity or DEM data at MVD. Also, bed sediment grain-size distributions for each MVD cross-section were characterized by only one bulk sample or one pebble count—further differentiations via facies mapping were not warranted. Finally, our method for extrapolating elevation changes at MVD cross-sections to estimate volumetric (and ultimately mass) changes for the bed material sediment budget was different: instead of extrapolating cross-section area changes over representative distances upstream and downstream as described above for Simkins, we estimated average cross-section elevation change and applied these over representative areas upstream and downstream (see *Pearson et al.* (2011) for details). The different extrapolation methods have comparable measurement errors and thus do not significantly affect our sediment budget comparisons.

The MVD data presented here document ongoing geomorphic response to dam removal beyond the near-term response reported by *Pearson et al.* (2011) for

the period from breach to May 2010. We continued to monitor geomorphic change with surveys in June 2011, July 2012, and July 2014 using the methods of *Pearson et al.* (2011). Minor differences (<4%) between our sediment budget calculations and those reported by *Pearson et al.* (2011) reflect refinement of the methods used to account for changes between surveys. *Conlon* (2013) provides further details about the 2011 and 2012 field campaigns.

**Results**

*Simkins impoundment response*

Simkins Dam removal began on November 24, 2010, and in less than a week the 3 m elevation spillway was removed to base level—the pre-dam channel bed. The stored sediment incised rapidly to nearly base level in the lower impoundment, as recorded by the first post-removal survey at XS-4 in February 2011 (Figure 5a). In the upper impoundment, incision was slower but nonetheless mostly complete at XS-2 by April 2011 (Figure 5b). Incision was accompanied, or succeeded, by channel widening throughout the impoundment. Rapid erosion is also evident in plots of cumulative cross-section area change (Figure 6b) and the bed material budget, which shows that over 40% of the impounded sediment was eroded within about three months (Table 2). Erosion rates during this period, a time of very low flows on the river (Figure 7b), were more than 60% greater than any other time interval (Table 2). Erosion rates remained substantial through the September 2011 survey, by which time more than 80% of the total stored sediment had been eroded from the impoundment, aided by an approximately 10-year recurrence interval event on September 7 associated with Tropical Storm Lee (Figure 7b). Episodic erosion

occurred throughout the remainder of the study period and only about 5% of the impounded sediment remained by the November 2013 survey (Table 2).

Channel bed grain size coarsened in the former Simkins impoundment as sand-sized sediments were eroded and the pre-dam, gravel-bedded, Piedmont channel was exhumed. This evolution is most evident in the lower impoundment. Figure 6a shows persistent coarsening from sand-size to pebble-sized $D_{50}$ for the dominant facies of the lower two cross-sections. The $D_{50}$ of the dominant facies in the upper impoundment also increased from medium sand to pebbles, but late in the study period these upper reaches were modestly aggraded with finer materials from farther upstream so that coarse sands were the $D_{50}$ of the dominant facies by November 2013.

*Downstream response: Simkins Dam to Bloede Dam reach*

Figure 4b shows that the Simkins Dam removal temporarily elevated turbidity at the Catonsville gage above levels recorded simultaneously at the Hollofield control gage. However, the comparative turbidity records also show that the turbidity spike shortly after dam removal was of a similar magnitude and duration to turbidity peaks produced at both gages by watershed stormflows unaffected by dam removal. Hollofield turbidity is unaffected by the dam removal throughout the period shown in Figure 4b and the removal's influence on turbidity at Catonsville probably does not extend beyond 2011.

The dominantly sand-sized sediments that were rapidly eroded from the Simkins impoundment during the first three months following dam removal aggraded the free-flowing reach immediately downstream and the upper Bloede impoundment by as much as 1.5 m over the same period (Figure 5c and d). Inspection of the

sediment budget shows that virtually all of the sediment eroded by February 2011 was trapped in this reach (Table 2 and Figure 7c). Between February and April 2011, additional sediment was released from the Simkins impoundment and some sediment that had aggraded in the free-flowing section in the first three months (Figure 5c) was remobilized and redeposited in the Bloede impoundment (Figure 5d) by small storms and base flows. Tropical Storm Lee in September 2011 accelerated sediment redistribution in the reach and transported the first substantial quantity of Simkins sediment over Bloede Dam (Table 2, Figures 5c-d, 6b, and 7b). Outputs over the dam in successive surveys reflected modest erosion from the Simkins impoundment and remobilization of sediment stored temporarily above Bloede Dam (Table 2 and Figure 6b). By April 2012, erosion in the free flowing reach above the Bloede impoundment had reestablished the pre-removal channel dimensions (Figure 5c and 6b) but a significant quantity of Simkins sediment remained stored in the Bloede impoundment by November 2013 (Table 2, Figure 5d and 6b).

Channel bed texture ranged widely throughout the study period immediately downstream of the Simkins Dam site as the cobble bed was first aggraded with sand and subsequently re-exposed (Figure 6a). The full range of texture change at XS-5, the first section below the Simkins Dam, was not captured quantitatively because our first post-removal facies mapping and sediment sampling did not occur until July 2011. By that time, the $D_{50}$ of the dominant facies was back in the gravel range because some coarser bed materials were rapidly re-exposed by erosion of the sand (Figure 5c). Texture change in the Bloede impoundment was generally smaller. XS-6, at the upper boundary of the impoundment, fined considerably from a pebble-sized $D_{50}$ to coarse sand, but farther downstream the changes were more modest with a shift from fine-medium sands to coarse sands (Figure 6a).

*Downstream response: Below Bloede Dam*

The Tropical Storm Lee flood of 7 September 2011 moved Simkins reservoir sediment downstream of Bloede Dam, leaving an irregular mantle of sand, most persistently in the reach near the Fall Line where the channel gradient flattens from 0.002 to 0.0004 (5-8 km downstream of Simkins Dam; Figure 6a and b). Cross-sections here (not shown) and DEMs (Figure 3c) recorded about 0.3 m to a maximum of about 1 m of aggradation over the study period and $D_{50}$ of the dominant facies shifted from pebble-sized to coarse-very coarse sands (Figure 6a). Farther downstream in the sand-bedded, Coastal Plain reach, aggradation was more modest and at one section there was minor net degradation (Figure 6b). Changes in $D_{50}$ of the dominant facies were also more modest and variable, with most sections beginning and ending the study period in the sand range (Figure 6a).

*Ongoing response at MVD: 2010-2014*

The May 2010 survey by *Pearson et al.* (2011) showed that less than 25% of the original sediment mass remained in the former impoundment nearly two years after removal. The next survey in June 2011 found virtually no change, but surveys in July 2012 and July 2014 documented further evacuation of 3% and 4%, respectively, of the stored sediment such that ~ 17% of the original mass remained (Figure 7c). The most visible change in the impoundment during the period was a thalweg shift between June 2011 and July 2012 from the right to left side of the mid-impoundment island where most of the remaining impoundment sediment is stored (*Conlon,* 2013). By 2014, some new sediment had deposited in places on both the left and right sides of the former impoundment, suggesting stabilization of the channel had begun to occur. In particular, several >20 m tall trees were recruited

from the left terrace during the March 2010 flood, and these created a platform for deposition outside of the active channel.

Despite the net delivery of sediment from upstream during the period 2010-2014, the downstream reach for the same period showed modest, net export of the sediments deposited, and temporarily stored, since removal (~ 10%; Figure 7c). As described by *Pearson et al.* (2011), this short reach of river (~ 0.5 km) between the dam site and the Merrimack River confluence has historically been highly dynamic because of episodic sediment delivery from upstream (including pulses delivered over the dam before removal; (*Pearson and Pizzuto,* 2015)), deposition enhanced by periodic backwatering from the larger Merrimack River, and subsequent remobilization over longer periods during modest flows. This dynamism persisted during the 2010-2014 period and was evident in localized, active erosion and deposition at the four downstream cross-sections.

## Discussion

Our paired analyses of the similar case studies at the Patapsco and Souhegan rivers reveal some important commonalities in initial versus longer-term responses to abrupt increases in sediment supply (Figure 7). At both sites, rapid evacuation of impoundment sediment occurred in the absence of large discharges (floods with annual recurrence intervals greater than 5 years; hereafter "$Q_5$") in the days and weeks following dam removal. $Q_5$ flood events are generally larger than channel-forming, or "effective", discharges (*Wolman and Miller*, 1960). During this "process-driven" phase, *Pearson et al.* (2011) proposed that the energy from base level change is sufficient to sustain erosion without large floods. Put another way, immediately after dam removal, the large sand supply in the former impoundment

leads to end-member transport-limited conditions as a new channel forms. The Simkins site demonstrates this phenomenon particularly well given the small discharge in the first few months after removal (Figure 7b).

After several months, and with about 50% of the impoundment sediment remaining, both sites appear to transition to the proposed "event-driven" phase when discharges >$Q_5$ become necessary to overtop the incised channel banks and erode the remaining, more distal sediment supply. A channel had formed through each impoundment and incision to base level was mostly complete in the reach closest to the dam site (e.g., Figure 5a). At MVD, an estimated 10-yr recurrence interval flow (based on nearly 100 years of record; Figure 7a) occurred at nearly 600 days post-removal and eroded 16% of the total impounded sediment (Figure 7c; after *Pearson et al.*, 2011). Subsequent annual peaks that were smaller eroded much less. Tropical Storm Lee delivered a 10-yr event to the Simkins site approximately 300 days after dam removal and, together with a smaller annual peak later that fall, removed 26% of the total impoundment sediment (Figures 7b and c and Table 2). Little further erosion was accomplished at Simkins until the next annual peak of comparable magnitude occurred at about 800 days, estimated to be between a 5 and 10-year recurrence interval event.

The Simkins erosion data generally indicate the change in process that characterizes the two-phase erosion model proposed by *Pearson et al.* (2011) for MVD. But it is not obvious from Figure 7c that the two erosion curves are not instead exhibiting continuous exponential decay with a single rate constant. To evaluate this, in Figure 8 we replot the erosion data for the MVD and Simkins impoundments and fit to the respective data series single-phase, non-linear least squares exponential models of the form:

$$N(t) = N_0e^{-\lambda t} \tag{2}$$

$N(t)$ is the quantity of impounded sediment remaining at any given time, $t$, in percent. $N_0$ is the intercept, or the quantity at $t=0$, which was set to 100% for each site to represent the sediment quantity impounded at the time dam removal began. As shown by *Pearson et al.* (2011) using a different fitting algorithm, the continuous exponential model (solid grey) appears to fit the MVD data poorly (Table 1 and Figure 8a). It underpredicts actual erosion in the early post-removal period and overpredicts later in the period. The single-phase exponential model fit to the Simkins data does a better job, especially for the early post-project period, but it also overpredicts the later stage (Table 1 and Figure 8b).

The single-phase exponential fit to the Simkins data prompted us to explore the idea that the proposed two-phase model and exponentially decreasing erosion rates are not mutually exclusive. The response rates in a two-phase process should still be related to the supply available for erosion, so we hypothesized that the process shift evident in our erosion data may be manifest in two-phase exponential decay models with changing decay constants ($\lambda$).

We fit two-phase, non-linear least squares exponential models to each impoundment erosion time series of the form:

$$N(t) = N_0e^{-(\lambda a)t} + N_1e^{-(\lambda b)t} \tag{3}$$

$N(t)$, $N_0$, and $t$ are as described above, $\lambda a$ and $\lambda b$ are decay constants for the two phases, and $N_1$ is the intercept for the second phase. $N_1$ is set to correspond to

when we estimate the process shift occurs: incision has reached base level at the dam and in the proximal areas upstream and the event-driven phase begins. Occurring at 52% and 45% of impounded sediment remaining at MVD and Simkins, respectively, these data points are shown as red circles in Figures 8a and b that correspond in time to red profiles plotted in the insets for representative cross-sections (as do other colored data points). Inspection of the four colored data point/profile pairs in each panel shows that the impoundments are indeed incised to base level, or near base level, at red and further significant erosion does not occur until sediments stored outside of the newly-formed channel are accessed (blue and green in Figures 8a and b, respectively). In our two-phase models, $N_1$ is set at 50% remaining for both sites because of the uncertainty associated with exactly when base level was achieved at each location (Table 1).

The two-phase model is clearly better than the single-phase model for the MVD data (Table 1 and Figure 8a). The process shift when base level is attained is manifest in an order of magnitude decrease in the decay constant from the first to second phase. Although the second phase of the model does not fit the data as well as the first phase, the residuals have a straightforward interpretation. Negative residuals (greater than expected erosion) follow intervals with erosion-producing events ($>Q_5$). Periods without events are characterized by successive data points that typically end with positive residuals (less than expected erosion; see period 1,000 to 2,200 days since breach on Figure 8a). Erosion during the event-driven phase is episodic and depends on the arrival rate of large discharges.

At Simkins, the two-phase process is less obvious. The occurrence of a ~10-year event at about 300 days, soon after incision to base level, partially obscures the phase transition (Figures 7 and 8b). Nonetheless, the two-phase exponential model

has a substantially improved fit compared to the single-phase model (change in AIC of 10; Table 1) and the same general pattern is evident: the decay constant decreases by 75% from the first to second phase and we see a second phase fit that is poorer than the first phase fit (Figure 8b). The event-phase residuals have the same interpretation as they do at MVD: negative residuals follow erosion-producing events and periods without events are characterized by successive data points ending with positive residuals (period 580 to 800 days since breach on Figure 8b).

The difference in valley width between the two sites may play a significant role in muting the evidence for the process shift at Simkins. If the event-phase is distinguished by the need for large floods to access sediments outside of the new channel, then we should expect a diminished effect in a confined valley setting where impounded sediments were stored comparatively close (compare Figure 8a and b insets). More rapid and complete erosion at the Simkins site in the event-driven phase may also be influenced by differences in local channel gradients and hydrologic response. The Patapsco River local to the dam is steeper than the Souhegan River and the comparatively flashier Patapsco River hydrograph also reflects the better integrated drainage network of its older landscape and more intense rainfall events in the Mid-Atlantic region (Table 1 and Figures 7a and b).

A similar two-phased erosion response has been observed at dam-removal sites in a variety of physiographic and climatic settings, including sites with larger dams impounding larger quantities of unconsolidated sediments (Major et al., Geomorphic responses to U.S. dam removals—a two-decade perspective, in press at Gravel Bed Rivers 8, 2017). *Major et al.* (2012) documented rapid erosion during modest flows evacuating greater than 40% of the 750,000 m$^3$ of sediments stored upstream of Oregon's Marmot Dam, even though about half of the impounded

sediments there were gravel-sized. Later erosion required larger flow events. Even

at the staged removals on the Elwha River, the largest dams removed in the world to

date, about one third of the total impounded sediment volume of 21 million m$^3$ was

released during the first two years when river discharges never exceeded the 2-yr

flood magnitude (*Magirl et al.*, 2015; *Randle et al.*, 2015; *Warrick et al.*, 2015). This

quantity represents about 40 years of watershed sediment supply (*Randle et al.*,

2015). A recent flume study of staged dam removal also observed that much of the

sediment erosion occurs soon after dam removal regardless of flow magnitude

(*Ferrer-Boix et al.*, 2014).

Downstream the responses at the two sites were more divergent. *Pearson et

al.* (2011) show how aggradation of up to 3 m that occurred in the days following

dam removal at MVD was enhanced by backwater effects of a high stage on the

considerably larger Merrimack River ~0.5 km downstream. The maximum

downstream storage of released sediments, about 30%, occurred during this period.

This temporarily steepened the downstream reach considerably, which subsequently

promoted, along with reduced stage on the Merrimack River, remobilization and

transport of sediments delivered from the impoundment later in the process-driven

period (Figure 7c). In contrast, Bloede Dam provided a persistent grade control in the

reach below Simkins Dam that supported longer duration storage (Figure 7c).

Though sediments aggraded in the free-flowing section immediately downstream of

Simkins Dam were subsequently remobilized by later flows (Figure 5c), the Bloede

impoundment served as an effective sediment detention basin, storing up to 50% of

the Simkins sediment. Three factors likely explain the greater trap efficiency of the

downstream reach at the Simkins site: (1) lower gradient in the Bloede

impoundment; (2) more complete erosion of the Simkins impoundment and resupply

of the downstream reach; and (3) lower base flows. Sand-sized sediments, which move as bedload even during modest flows, are transported more effectively through the downstream reach at the MVD site by more robust base flows compared to the Simkins site (Table 1 and Figures 7a and b).

In the longer reach below Bloede Dam, for which there is no analog at MVD, persistent aggradation near the Fall Line reflects the resupply of sediment from the Bloede impoundment and the change in channel gradient. We suspect the aggradation and dominance of sand-sized facies there will continue until the Simkins sediment detained in the Bloede impoundment is remobilized and exhausted.

**Conclusions**

Dam removals with uncontrolled sediment releases are valuable opportunities to investigate channel response to abrupt increases in bed-material supply. The Simkins Dam removal provided an opportunity for a paired analysis where we could directly evaluate whether the two-phased impoundment erosion observed at MVD was repeatable, suggesting a more general fluvial response to these events. We found good correspondence between the erosion trajectories at the two sites with the process-driven phase exceptionally well demonstrated at Simkins given the low flows there in the months immediately after removal. Erosion during this time was driven by the increased energy slope caused by base level lowering, as well as the large supply of exposed sand. The subsequent event-driven phase began at both sites when approximately 50% of the impounded sediment mass had been eroded and further erosion depended on large floods ($>Q_5$) to access sediment stored outside of the new channel. We found the two-phase process could be described by two-phase exponential models with changing decay constants associated with the process

change, but this process shift was muted in the more confined valley of the Simkins site. Interestingly, valley confinement does not appear to be as important as gradient and base flow for the downstream response except indirectly through its influence on resupply from the upstream impoundment.

Rapid erosion of noncohesive sediments soon after removal has been identified as a key finding of the comparatively few dam-removal studies to date, suggesting rivers are resilient to dam removals (*O'Connor et al.*, 2015). The repeatability of the MVD results at Simkins adds strong supporting evidence for the two-phase disturbance response model that begins with this rapid erosion phase, and we further show that such a model does not conflict with earlier models proposing exponential decay of fluvial response rates. River resilience to dam-removal sediment releases is encouraging given the opportunities for dam removal to simultaneously address aging infrastructure concerns and a host of environmental and human use issues caused by dam emplacement (*Graf*, 2006; *Doyle et al.*, 2008). As exemplified by the findings of *Gran et al.* (2011), who documented changing process controls over time when investigating channel response to a volcanic eruption, what we are learning from dam-removal sediment releases also has applicability to abrupt sediment-supply increases caused by other disturbances including landslides.

## Acknowledgements and Data

Any use of trade, firm, or product names is for descriptive purposes only and does not imply endorsement by the U.S. Government.

## References

Baker DB, Richards RP, Loftus TT, Kramer JW. 2004. A new flashiness index: characteristics and applications to midwestern rivers and streams. Journal of the American Water Resources Association (JAWRA) 40(2): 503-522. DOI:10.1111/j.1752-1688.2004.tb01046.x

Bonnin GM, Martin D, Lin B, Parzybok T, Yekta M, Riley D. 2006. Precipitation-frequency Atlas of the United States, NOAA Atlas 14, Volume 2, Version 3.0. NOAA, National Weather Service: Silver Spring, Maryland

Bountry JA, Lai YG, Randle TJ. 2013. Sediment impacts from the Savage Rapids Dam removal, Rogue River, Oregon. Reviews in Engineering Geology 21: 93-104. DOI:10.1130/2013.4121(08)

Cleaves ET, Edwards Jr. J, Glaser JD. 1968. Geologic Map of Maryland. Maryland Geological Survey: Baltimore, Maryland.

Collins MJ, Kirk JP, Pettit J, DeGaetano AT, McCown MS, Peterson TC, Means TN, Zhang X. 2014. Annual floods in New England (USA) and Atlantic Canada: synoptic climatology and generating mechanisms. Physical Geography 35(3): 195-219. DOI:10.1080/02723646.2014.888510

Conlon M. 2013. A Hindcast Comparing the Response of the Souhegan River to Dam Removal with the Simulations of the Dam Removal Express Assessment

Model-1. M.S. thesis, Dept. of Earth and Env. Sciences, Boston College: Boston, MA.

Costa JE. 1975. Effects of agriculture on erosion and sedimentation in the Piedmont province, Maryland. Geological Society of America Bulletin 86: 1281–1286. DOI: 10.1130/0016-7606(1975)86<1281:EOAOEA>2.0.CO;2

DeGaetano A, Zarrow D, N.R.C. Center. 2011. Extreme Precipitation in New York & New England, Technical Documentation and User Manual. Northeast Regional Climate Center, Cornell University: Ithaca, NY.

Doyle MW, Stanley EH, Havlick DG, Kaiser MJ, Steinbach G, Graf WL, Galloway GE, Riggsbee JA. 2008. Aging infrastructure and ecosystem restoration. Science 319: 286-287. DOI: 10.1126/science.1149852

East AE, Pess GR, Bountry JA, Magirl CS, Ritchie AC, Logan JB, Randle TJ, Mastin MC, Minear JT, Duda JJ, Liermann MC, McHenry ML, Beechie TJ, Shafroth PB. 2015. Large-scale dam removal on the Elwha River, Washington, USA: River channel and floodplain geomorphic change. Geomorphology 228: 765-786. DOI:10.1016/j.geomorph.2014.08.028

Ferrer-Boix C, Martín-Vide JP, Parker G. 2014. Channel evolution after dam removal in a poorly sorted sediment mixture: Experiments and numerical model. Water Resources Research 50(11): 8997-9019. DOI: 10.1002/2014WR015550

Graf WL. 1977. The rate law in fluvial geomorphology. American Journal of Science 277(2): 178-191. DOI:10.2475/ajs.277.2.178

Graf WL. 2006. Downstream hydrologic and geomorphic effects of large dams on American rivers. Geomorphology 79(3): 336-360. DOI:10.1016/j.geomorph.2006.06.022

Grams PE, Topping DJ, Schmidt JC, Hazel JE, Kaplinski M. 2013. Linking morphodynamic response with sediment mass balance on the Colorado River in Marble Canyon: Issues of scale, geomorphic setting, and sampling design. Journal of Geophysical Research: Earth Surface 118(2): 361-381. DOI:10.1002/jgrf.20050

Gran KB, Montgomery DR, Halbur JC. 2011. Long-term elevated post-eruption sedimentation at Mount Pinatubo, Philippines. Geology 39(4): 367–370. DOI:10.1130/G31682.1.

Hack JT. 1960. Studies of Longitudinal Stream Profiles in Virginia and Maryland. U.S. Geological Survey Professional Paper 294-B. U.S. Government Printing Office: Washington, D.C.

Hershfield DM. 1961. Rainfall Frequency Atlas of the United States for Durations from 30 Minutes to 24 Hours and Return Periods from 1 to 100 years. Weather Bureau Technical Paper No. 40. U.S. Weather Bureau: Washington, D.C., 115 pp.

Kieffer SW. 1985. The 1983 hydraulic jump in Crystal Rapid: Implications for river-running and geomorphic evolution in the Grand Canyon. Journal of Geology 93(4): 385–406. DOI: 10.1086/628962

Kondolf GM, Matthews WV. 1991. Unmeasured residuals in sediment budgets: a cautionary note. Water Resources Research 27(9): 2483-2486. DOI: 10.1029/91WR01625

Larsen IJ, Schmidt JC, Martin JA. 2004. Debris-fan reworking during low magnitude floods in the Green River canyons of the eastern Uinta Mountains, Colorado and Utah. Geology 32: 309–312. DOI: 10.1130/G20235.1.

Magilligan FJ, Nislow KH, Kynard B, Hackman A. 2015. Immediate changes in stream channel geomorphology, aquatic habitat, and fish assemblages following dam removal in a small upland catchment. Geomorphology 252:158-170. DOI:10.1016/j.geomorph.2015.07.027

Magirl CS, Hilldale RC, Curran CA, Duda JJ, Straub TD, Domanski M, Foreman JR. 2015. Large-scale dam removal on the Elwha River, Washington, USA: Fluvial sediment load. Geomorphology 246: 669-686. DOI:10.1016/j.geomorph.2014.12.032

Major JJ, Pierson TC, Dinehart RL, Costa JE. 2000. Sediment yield following severe volcanic disturbance—a two-decade perspective from Mount St. Helens. Geology 28(9): 819-822. DOI:10.1130/0091-7613(2000)28<819:SYFSVD>2.0.CO;2

Major JJ, O'Connor JE, Podolak CJ, Keith MK, Grant GE, Spicer KR, Pittman S, Bragg HM, Wallick JR, Tanner DQ, Rhode A, Wilcock PR. 2012. Geomorphic Response of the Sandy River, Oregon, to Removal of Marmot Dam. U.S. Geological Survey Professional Paper 1792, 64 p.

Maryland Department of Natural Resources Watershed Services (MDNRWS). 2005. Characterization of the Patapsco River Lower North Branch Watershed in Howard County, Maryland. 21 p.

McGreevy LJ, Wheeler JC. 1985. Maryland and the District of Columbia. In National Water Summary 1984; Hydrologic Events, Selected Water-quality Trends, and Groundwater Resources. U.S. Geological Survey Water-Supply Paper 2275. U.S. Government Printing Office: Washington, D.C.; 243-248

Miller AJ. 1990. Flood hydrology and geomorphic effectiveness in the central Appalachians. Earth Surface Processes Landforms 15: 119–134. DOI: 10.1002/esp.3290150203

O'Connor JE, Duda JJ, Grant GE. 2015. 1000 dams down and counting. Science 348(6234): 496-497. DOI: 10.1126/science.aaa9204

Pearson AJ, Pizzuto J. 2015. Bedload transport over run-of-river dams, Delaware, USA. Geomorphology 248: 382-395. DOI: 10.1016/j.geomorph.2015.07.025

Pearson AJ, Snyder NP, Collins MJ. 2011. Rates and processes of channel response to dam removal with a sand-filled impoundment. Water Resources Research 47:W08504. DOI: 10.1029/2010WR009733.

Peel MC, Finlayson BL, McMahon TA. 2007. Updated world map of the Köppen-Geiger climate classification. Hydrology and Earth System Sciences 11: 1633-1644. DOI: 10.5194/hess-11-1633-2007

Pizzuto JE. 2002. Effects of dam removal on river form and process. BioScience 52(8): 683–691. DOI: 10.1641/0006-3568(2002)052(0683:EODROR)2.0.CO;2.

Randle TJ, Bountry JA, Ritchie A, Wille K. 2015. Large-scale dam removal on the Elwha River, Washington, USA: erosion of reservoir sediment. Geomorphology 246: 709-728. DOI: 10.1016/j.geomorph.2014.12.045

Rantz SE. 1982. Measurement and Computation of Streamflow: Volume 2, Computation of Discharge. U.S. Geological Survey Water-Supply Paper 2175. U.S. Government Printing Office: Washington, D.C.

Ries KG. 1997. August Median Streamflows in Massachusetts. U.S. Geological Survey Water-Resources Investigations Report 97-4190. Marlborough, MA

Smith JA, Baeck ML, Villarini G, Krajewski WF. 2010. The hydrology and hydrometeorology of flooding in the Delaware River Basin. Journal of Hydrometeorology 11: 841-859. DOI: 10.1175/2010JHM1236.1

Smith JA, Villarini G, Baeck ML. 2011. Mixture distributions and the hydroclimatology of extreme rainfall and flooding in the eastern United States. Journal of Hydrometeorology 12: 294–309. DOI: 10.1175/2010JHM1242.1

Smith SMC, Wilcock PR. 2015. Upland sediment supply and its relation to watershed sediment delivery in the contemporary mid-Atlantic Piedmont (U.S.A.). Geomorphology 232: 33-46. DOI: 10.1016/j.geomorph.2014.12.036

Stillwater Sciences. 2010. Simulating Sediment Transport in the Patapsco River following Dam Removal with Dam Removal Express Assessment Model-1 (DREAM-1). Prepared for Interfluve, Inc. and American Rivers.

Taylor JR. 1997. An Introduction to Error Analysis. University Science Books: Sausalito, CA

Tullos DD, Collins MJ, Bellmore JR, Bountry JA, Connolly PJ, Shafroth PB, Wilcox AC, 2016. Synthesis of common management concerns associated with dam removal. Journal of the American Water Resources Association (JAWRA) 52(5):1179–1206. DOI: 10.1111/1752-1688.12450

Warrick JA, Bountry JA, East AE, Magirl CS, Randle TJ, Gelfenbaum G, Ritchie AC, Pess GR, Leung V, Duda JJ. 2015. Large-scale dam removal on the Elwha River, Washington, USA: source-to-sink sediment budget and synthesis. Geomorphology 246: 729-750. DOI: 10.1016/j.geomorph.2015.01.010

Webb RH, Melis TS, Griffiths PG, Elliot JG. 1999. Reworking of aggraded debris fans. In The Controlled Flood in Grand Canyon, American Geophysical Union Geophysical Monograph 110, Webb RH et al. (eds). AGU: Washington, D.C.; 37–51

Wentworth CK. 1922. A scale of grade and class terms for clastic sediments. Journal of Geology 30(5): 377-392. DOI: 10.1086/622910

Wolman GM, Miller JP. 1960. Magnitude and frequency of forces in geomorphic processes. Journal of Geology 68: 54-74. DOI: 10.1086/626637.

**Tables**

Table 1: Study area attributes.

| | Simkins Dam | Merrimack Village Dam |
|---|---|---|
| *dam* | | |
| height | ~3 m | ~4 m |
| operation style | run-of-river | run-of-river |
| purpose | mill power | mill power |
| construction date | 1889[a,c] | 1907[b,c] |
| removal date | Fall 2010 | Summer/Fall 2008 |
| removal mechanism | mechanical (hoe ram) | mechanical (hoe ram) |
| stored sediment volume | ~ 67,000 m$^3$ | ~ 65,000 m$^3$ |
| stored sediment texture | dominantly sand | dominantly sand |
| | | |
| *physiography* | | |
| watershed area | 950 km$^2$ | 570 km$^2$ |
| gradient local to dam | 0.0017 | 0.0004 |
| impoundment max. wetted width | 55 m | 90 m |
| drainage density | 1.5 km$^{-1}$ | 1 km$^{-1}$ |
| | | |
| *hydrology* | | |
| base flow | 1.9 m$^3$/s | 3.5 m$^3$/s |
| mean annual discharge | 7.5 m$^3$/s | 8.4 m$^3$/s |
| mean annual flood | 400 m$^3$/s | 100 m$^3$/s |
| Richards-Baker flashiness | 0.41 | 0.24 |
| | | |
| *impoundment erosion rates*[d] | | |
| single-phase model | $N(t) = 100e^{-0.004t}$ | $N(t) = 100e^{-0.002t}$ |
| df, AIC[e] | 2, 47.3 | 2, 71.8 |
| two-phase model | $N(t) = 50e^{-0.009t} + 50e^{-0.002t}$ | $N(t) = 50e^{-0.032t} + 50e^{-0.001t}$ |
| df, AIC | 3, 37.5 | 3, 49.2 |

[a] Maryland Historical Trust, documentation for determination of eligibility.
[b] *Pearson et al.* (2011).
[c] Date of most recent dam at the site.
[d] These models are presented in Figure 8 and detailed in the Discussion. N(t) is the quantity of impounded sediment remaining at any given time, t, in percent.
[e] Degrees of freedom and Akaike information criterion, respectively.

Table 2: Bed material budget, Simkins impoundment to Bloede Dam.

| Survey | Days since breach | Input[a] | $\Delta S_{us}{}^{b}$ | Upstream remaining[c,d] | | Average erosion rate | $\Delta S_{ds}{}^{b}$ | Downstream cumulative storage[d] | | Output[e] | $\Delta S_{XS9\text{-}16}{}^{f}$ |
|---|---|---|---|---|---|---|---|---|---|---|---|
| | | (t) | (t) | (t) | (%) | (t/day) | (t) | (t) | (%) | (t) | (t) |
| Sep-2010 | 0 | 0 | 0 | 96,000 | 100 | 0 | 0 | 0 | 100 | 0 | |
| Feb-2011 | 112 | 2,000 | -39,000 ± 8,000 | 57,000 | 59 | 350 | 39,000 ± 8,000 | 39,000 | 141 | 2,000 | -5,000 ± 21,000 |
| Apr-2011 | 174 | 1,000 | -13,000 ± 10,000 | 44,000 | 45 | 210 | 11,000 ± 12,000 | 51,000 | 153 | 3,000 | 800 ± 21,000 |
| Sep-2011 | 419 | 4,000 | -25,000 ± 4,000 | 18,000 | 19 | 100 | -500 ± 5,000 | 50,000 | 152 | 30,000 | 27,000 ± 22,000 |
| Apr-2012 | 580 | 3,000 | -4,000 ± 3,000 | 14,000 | 15 | 30 | -500 ± 5,000 | 50,000 | 152 | 8,000 | -2,000 ± 21,000 |
| Nov-2012 | 784 | 3,000 | 200 ± 3,000 | 14,000 | 15 | 0 | -16,000 ± 6,000 | 33,000 | 135 | 19,000 | 13,000 ± 21,000 |
| Nov-2013 | 1220 | 7,000 | -10,000 ± 3,000 | 4,000 | 4 | 20 | 2,000 ± 5,000 | 36,000 | 137 | 15,000 | 18,000 ± 21,000 |

[a] Based on estimated annual rate of 5,700 t/yr (see Methods) that does not consider discharge for a given period.

[b] Reported errors for each survey not accumulated in these columns, with the exception of April 2011 when incremental storage change had to be computed using the storage change estimates for the February 2011 campaign (see text).

[c] Upstream remaining mass estimate at day 0 based on lower estimate by Interfluve, Inc. (unpublished data, 2009) and a bulk density of 1.43 g/cm³

[d] Cumulative storages in tonnes and percent calculated retaining one additional significant figure than ultimately reported in tonnes (percentages not rounded), thus calculations down column will not compute exactly. Errors reported in adjacent columns to the left accumulate after April 2011 (which is already accumulated per note b) so that by November 2013 the estimated Upstream remaining is ± 23,000 t and the Downstream cumulative storage is ± 33,000 t.

[e] Residual calculation

[f] Estimated changes in storage in the reach downstream of Bloede Dam to the USGS Elkridge gage. Estimates based on cross-section 9 through 16 measurements.

**Figures**
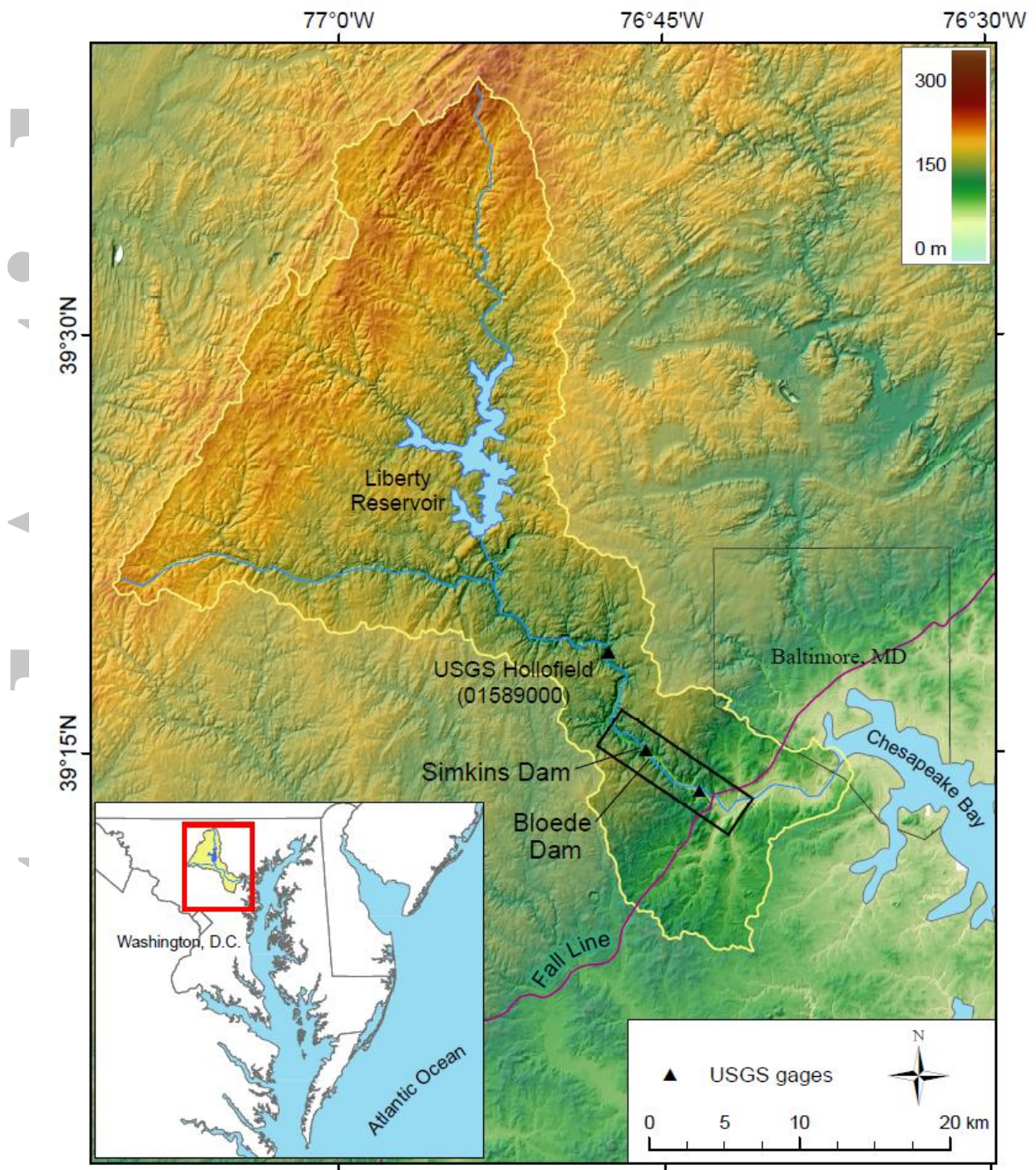


Figure 1: The Patapsco River watershed. Black extent rectangle delimits the Simkins Dam removal study area, detailed in Figure 3.

Figure 2: Simkins Dam before (a) and during (b) the late 2010 removal; Merrimack Village Dam (MVD) in 2003 (c) and during the 2008 removal (d).
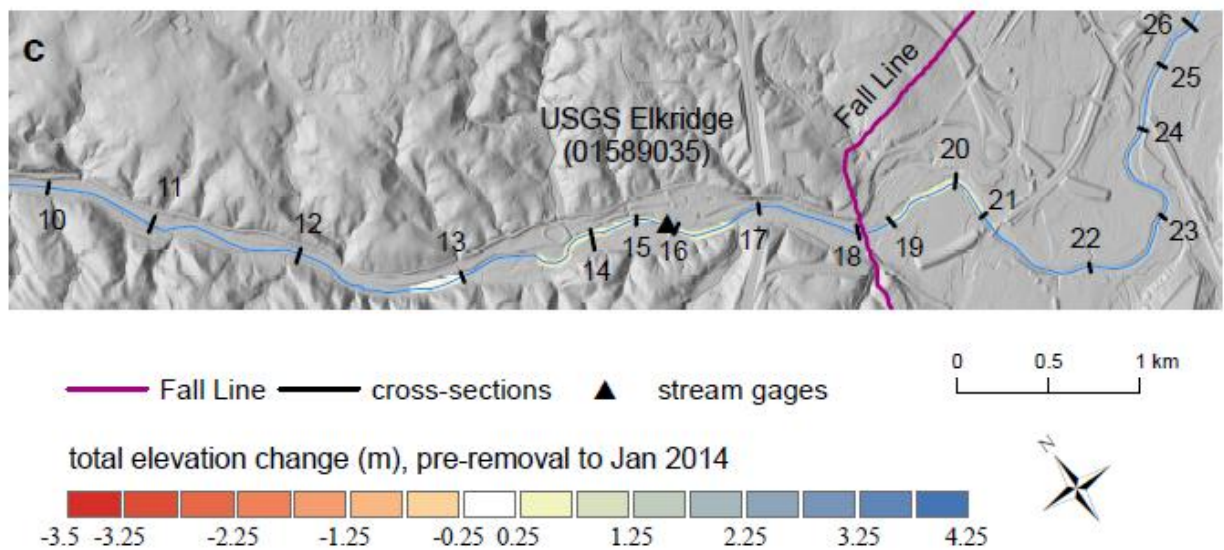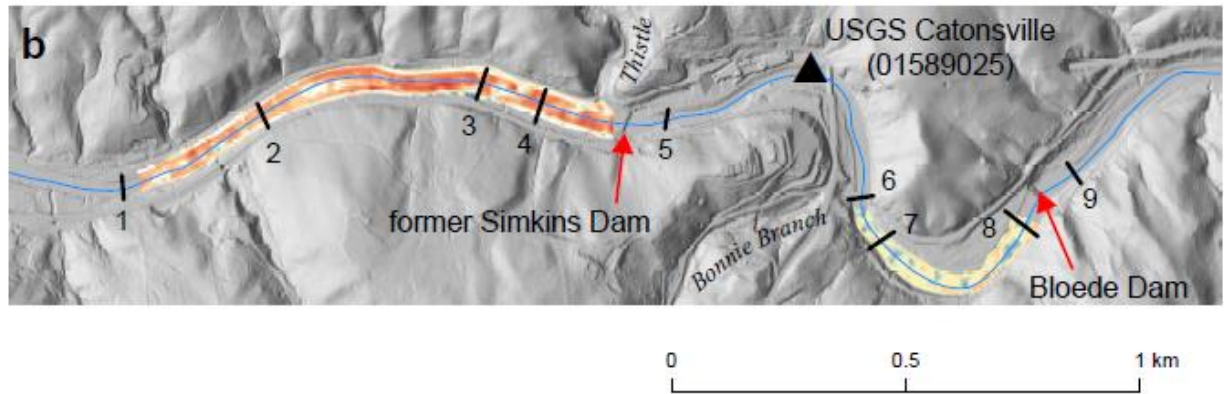
Figure 3: (a) Shaded relief of Patapsco study area showing extent rectangles for hillshades of (b) the upper study reach with the dam sites and (c) the lower reach where the channel transitions from comparatively steep (0.002) and confined in the Piedmont section to unconfined and low gradient (0.0004) in the Coastal Plain. Blue line is channel centerline approximated from pre-removal county lidar DEM mosaic. See Figure 1 for shaded relief elevation key.
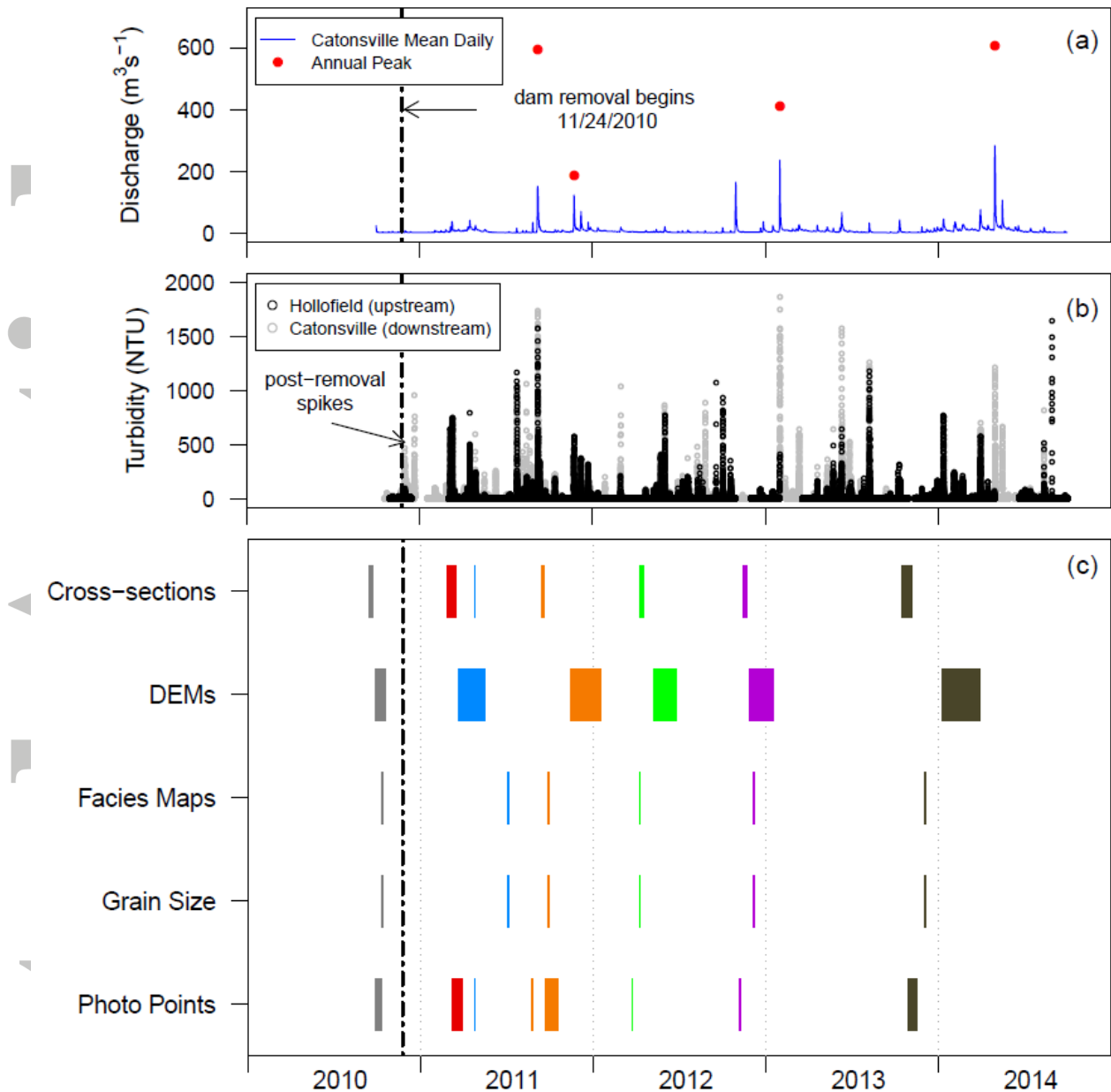
Figure 4: (a) Patapsco River hydrograph, (b) turbidity time series, and (c) morphometry data collection schedule. Field campaigns in lower panel are named by the month and year monumented cross-section surveys began: September 2010 (grey); February 2011 (red); April 2011 (blue); September 2011 (orange); April 2012 (green); November 2012 (purple); November 2013 (dark brown). For the April 2011 campaign (blue), cross-sections and photo points were collected only at a subset of the fixed stations for these parameters (XS-1 through XS-17); facies maps and grain size samples were not collected until July 2011. Turbidity time series shown in (b) are also shown in *Tullos et al.*, 2016.
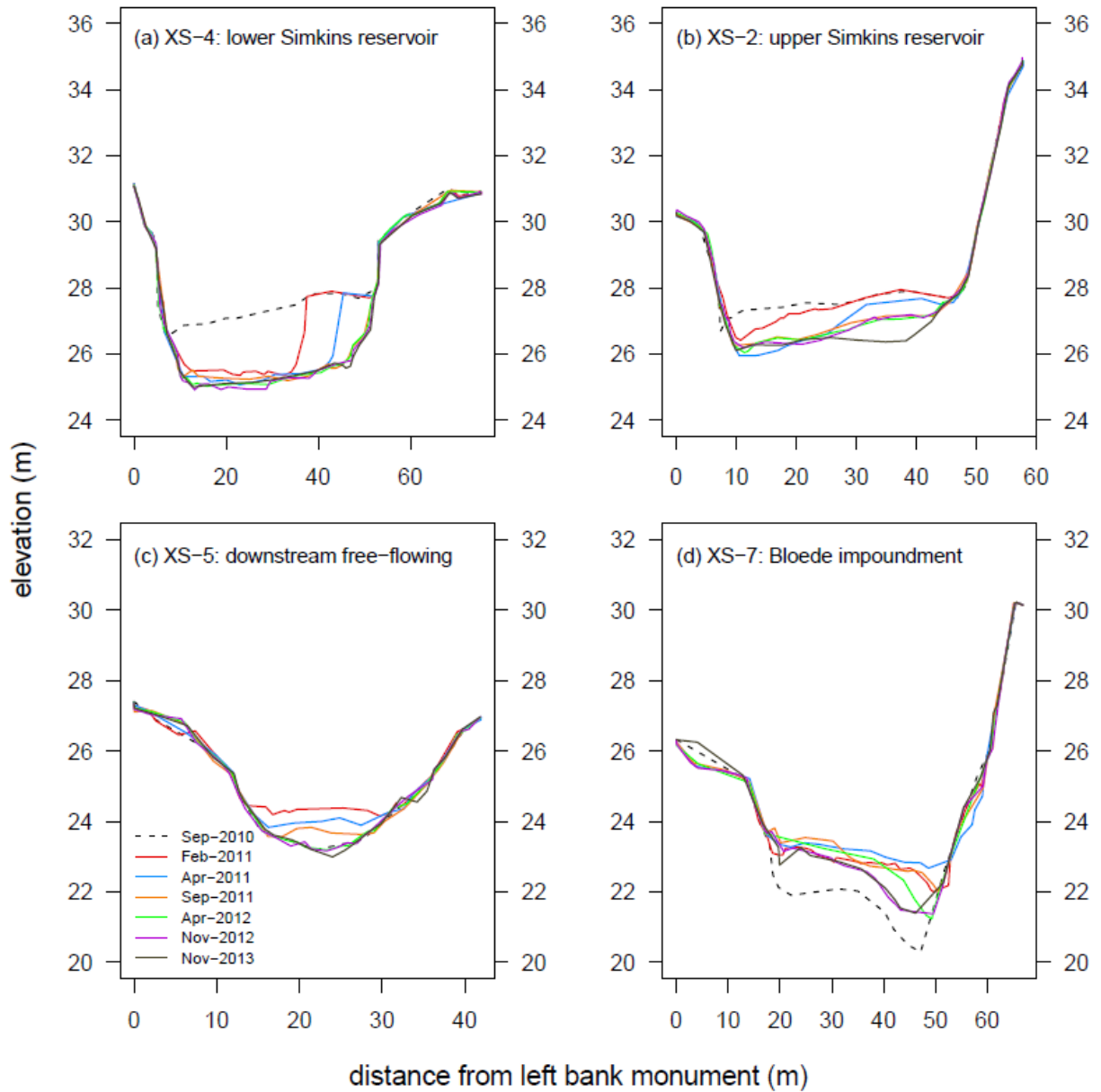
Figure 5: Example cross-section changes in the Simkins impoundment (a and b), the free-flowing reach immediately downstream (c), and the Bloede impoundment (d). Vertical datum is NAVD88.
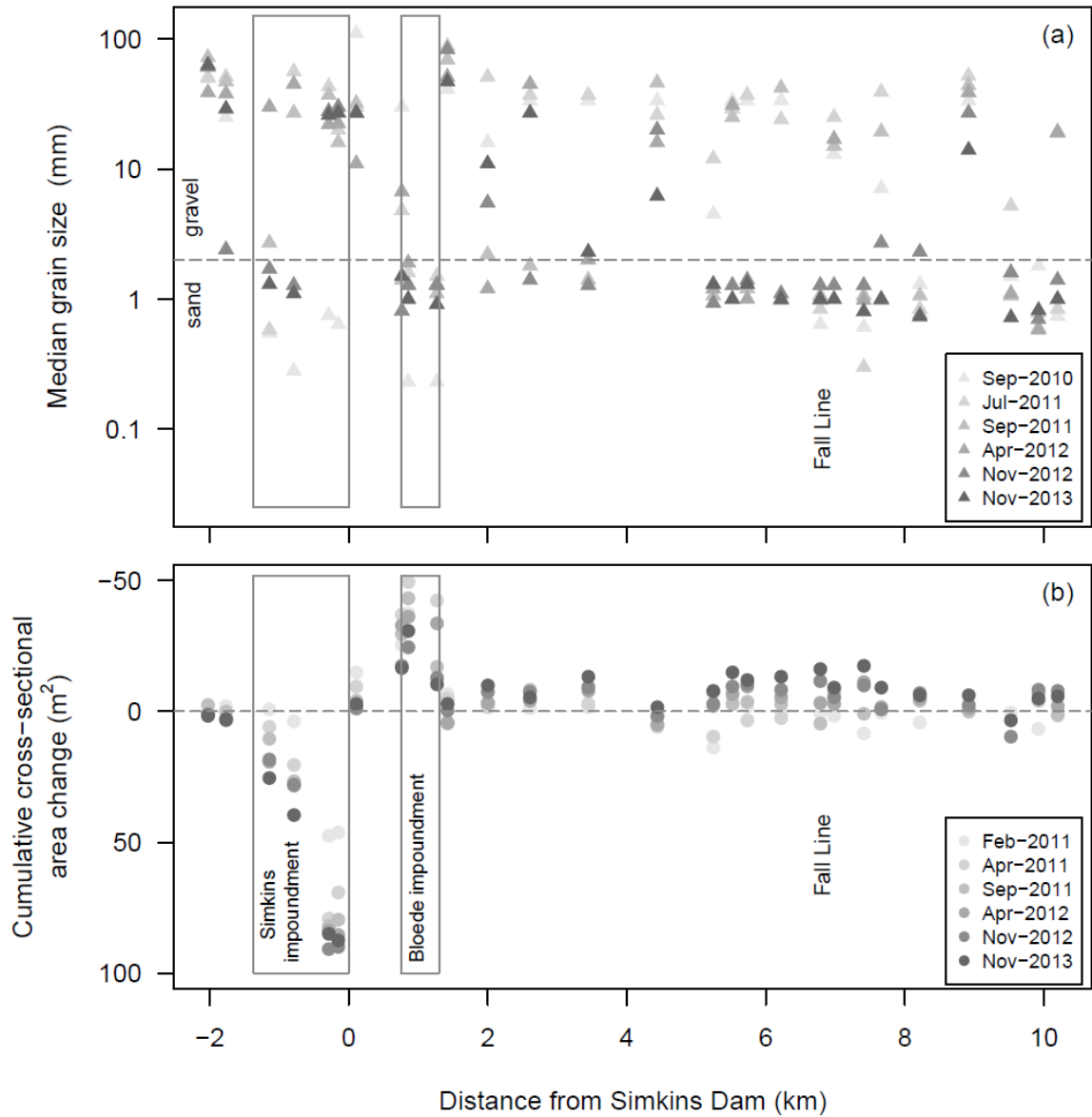
Figure 6: Temporal evolution of (a) dominant median grain size ($D_{50}$) and (b) channel capacity at the 28 monumented cross-sections throughout the Patapsco study area. Positive (negative) cumulative changes in channel cross-sectional area indicate the cumulative area of erosion (deposition) at a section.
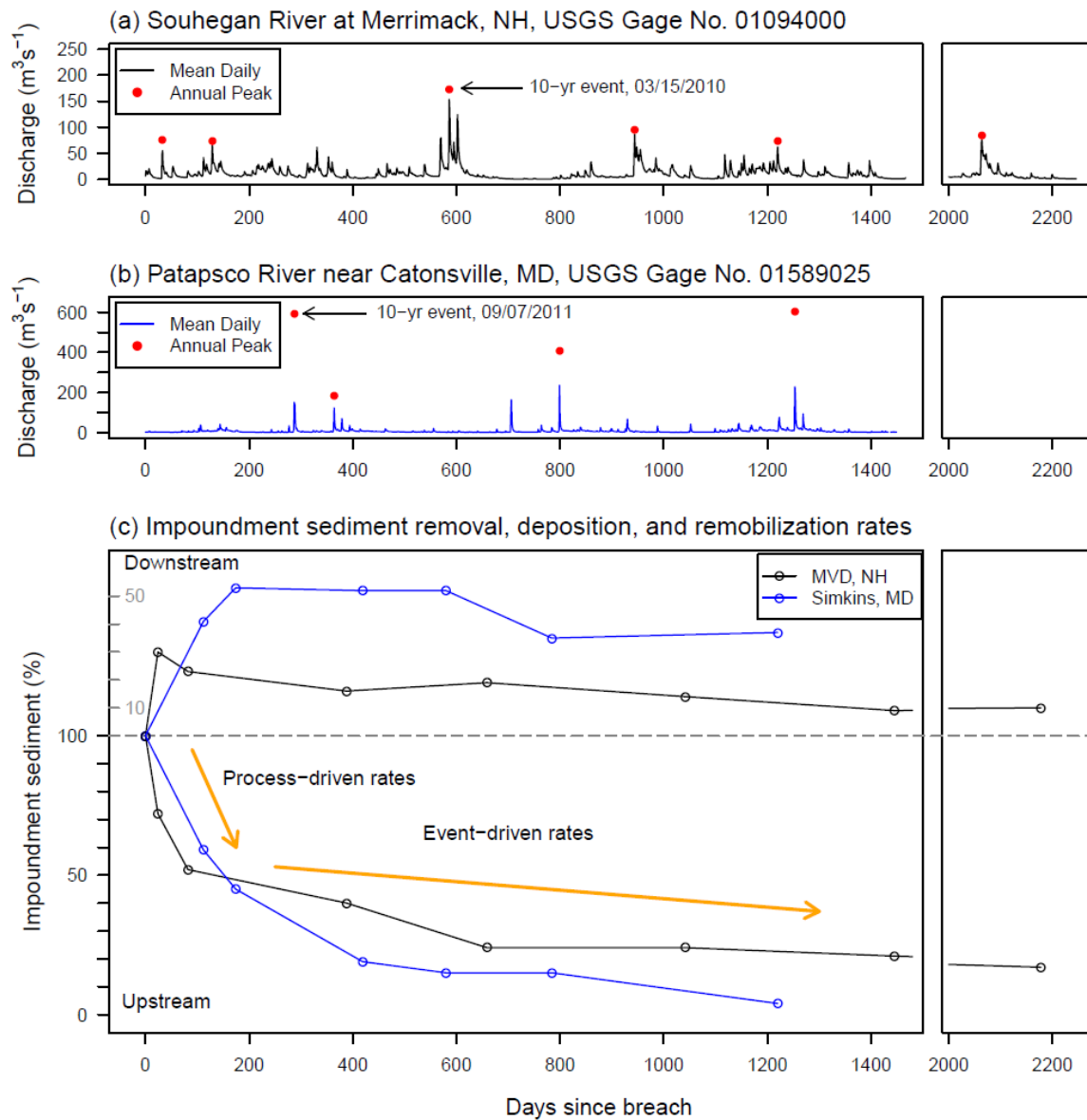
Figure 7: Post-removal hydrographs for the MVD site (a) and Simkins Dam site (b) along with their comparative erosion, deposition, and remobilization rates (c). Simkins erosion data in (c) also shown in review paper by Major et al. (Geomorphic responses to U.S. dam removals—a two-decade perspective, in press at Gravel Bed Rivers 8, 2017). MVD erosion data to ~700 days after *Pearson et al.* (2011).
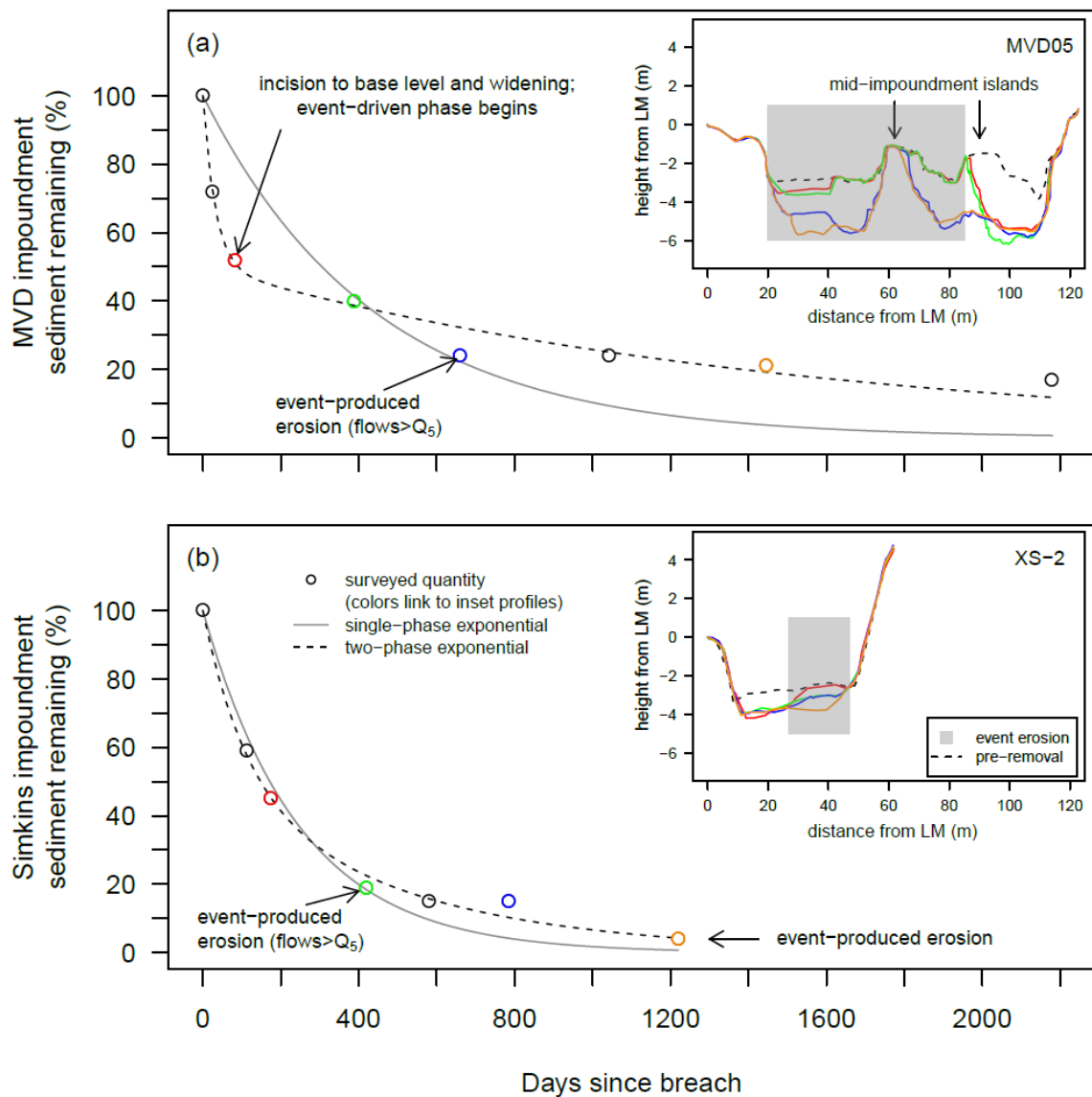
Figure 8: Measured quantities of impoundment sediment remaining with time (as in Figure 7c) plotted with single- and two-phase non-linear least squares exponential models fit to the data series. Colored data points correspond in time with profiles for representative cross-sections shown in the insets, where "LM" indicates "left monument". (a) MVD impoundment. (b) Simkins impoundment. The two fitted models for each site, and measures of their comparative fit, are shown in Table 1.